

Canonical strangeness suppression in microscopic transport models

O. Fochler, S. Vogel, M. Bleicher, C. Greiner, P. Koch-Steinheimer, and Z. Xu

Institut für Theoretische Physik, J.W. Goethe Universität, Max-von-Laue-Str. 1, D-60438 Frankfurt am Main, Germany

(Received 20 January 2006; published 6 September 2006)

We demonstrate the occurrence of canonical suppression associated with the conservation of a U(1) charge in current transport models. For this study a pion gas is simulated within two different transport approaches by incorporating inelastic and volume-limited collisions $\pi\pi \leftrightarrow K\bar{K}$ for the production of kaon pairs. Both descriptions can dynamically account for the suppression in the yields of rare strange particles in a limited box, being in full accordance with a canonical statistical description.

DOI: [10.1103/PhysRevC.74.034902](https://doi.org/10.1103/PhysRevC.74.034902)

PACS number(s): 24.10.Pa, 24.60.-k, 25.75.Dw

I. INTRODUCTION AND MOTIVATION

For many years the various properties of excited nuclear matter occurring in heavy collisions have been studied within statistical descriptions [1–6]. Here the underlying principle is the stringent assumption of full thermal equilibrium in the stage of the reaction to which the description is applied.

In the last 10 years thermal model ansatzes of hadronic resonance gases via a grand canonical description have become very popular again because detailed experimental results for the yields of individual hadronic species became available at various bombarding energies. Indeed, it was found that the statistical description can be applied very successfully for ultrarelativistic energies, indicating that the individual hadronic particles seem to evolve to a point of nearly perfect chemical equilibrium [7,8] (for a comprehensive review the reader is referred to [9]).

However, for low collision energies (e.g., in the GSI Schwerionensynchrotron (SIS), the BNL Alternating Gradient Synchrotron (AGS), and the GSI-FAIR range) especially the strange particles do become rare. Thus, as has been well known for a long time, a canonical instead of a grand canonical description of the strange particles must be applied. The canonical approach results in a suppression in the yields for rare particles in comparison to the grand canonical description when treating the conservation of the corresponding U(1) charge exactly [10–12]. Indeed, thermal models including the canonical suppression have been applied rather successfully for the description of the few measured hadronic yields in heavy ion collisions at SIS energies [13–15].

A dynamical interpretation of the canonical suppression has recently also been offered by the formulation and solution of kinetic master equations [16,17]. It is the purpose of this investigation to show that such an occurrence of canonical suppression for rare particles is already warranted by present day transport models.

A priori this is not a trivial statement. One could argue that the transport models are based on solving a set of coupled Boltzmann equations that originate from a grand canonical treatment. However, this is not the case as the realizations do conserve energy exactly and also the individual quantum charges like baryon number and (net) strangeness are conserved during the propagation and scattering processes as well.

In the following section we briefly review the canonical suppression of rare particles associated with the conservation of a U(1) charge and we also summarize its dynamical formulation via a master equation as given in [16,17]. In Sec. III we describe our simulation setup. A pion gas is simulated by incorporating inelastic and volume-limited collisions $\pi\pi \leftrightarrow K\bar{K}$ for the production of kaon pairs. We employ two completely different numerical realizations for the treatment of collisions. The first model under investigation is UrQMD [18,19], where two-particle collisions are realized via a standard geometrical interpretation. For previous studies of the thermodynamic properties of hadronic matter within the UrQMD model, the reader is referred to [20–23]. In the second model the collisions are treated by transition rates in small spatial subcells. The latter algorithm has most recently been successfully introduced in a covariant parton cascade to describe inelastic multiparticle Bremsstrahlung processes of type $gg \leftrightarrow ggg$ [24]. In Sec. IV we present the results of our analysis. Section V then provides a summary and a conclusion. We argue that a (canonical) chemical equilibrium of kaons cannot by far be achieved at intermediate energies for relativistic heavy ion collisions, at least if known cross sections for the production of kaons are assumed.

II. CANONICAL SUPPRESSION AND ITS DYNAMICAL DESCRIPTION VIA A MASTER EQUATION

The statistical description of systems incorporating the exact conservation of quantum numbers has been established for many years and there exist several approaches of varying complexity and generality [10–12]. Here we give a brief summary of the results adapted to our needs. The conserved U(1) charge to be considered is strangeness whose net value is taken to be zero throughout our calculations and simulations. Explicitly we consider only inelastic reactions of the type $\pi\pi \leftrightarrow K\bar{K}$, where the kaons and antikaons bear strangeness +1 and -1, respectively.

For a large number of kaons it is sufficient to treat strangeness conservation on the average $\langle N_K \rangle - \langle N_{\bar{K}} \rangle = 0$ (with $N_K, N_{\bar{K}}$ being the number of kaons and antikaons, respectively). Introducing a chemical potential μ_s , or fugacity $\lambda_s = \exp(\frac{\mu_s}{T})$, to control the net strangeness content, one is led

to the following grand canonical partition function

$$Z^{\text{gc}}(V, T, \lambda_s) = \exp(Z_\pi^1 + \lambda_s Z_K^1 + \lambda_s^{-1} Z_{\bar{K}}^1), \quad (1)$$

where Z_i^1 denotes the relativistic one-particle partition function for noninteracting particles of type i (pions or kaons in this case), V is the volume, T is the temperature, and m_i is the particle's mass. K_2 denotes a modified Bessel function.

$$Z_i^1(V, T) = g_i \frac{VT}{2\pi^2} m_i^2 K_2\left(\frac{m_i}{T}\right). \quad (2)$$

To consider a more general case, the one-body partition functions in (1) would have to be replaced by sums over one-body partition functions of all hadronic particles carrying the corresponding integer in strangeness of 0, ± 1 , ± 2 , and ± 3 .

A small number of kaons (roughly spoken when the average number becomes of order one) demands the conservation of strangeness to be treated exactly, i.e., $N_K - N_{\bar{K}} = 0$ for each state contributing to the partition sum. This constraint leads to a reduction of the available phase space for the production process and ultimately one obtains the canonical partition function describing the system via (I_0 and I_1 denote Bessel functions)

$$Z^c(V, T) = \exp(Z_\pi^1) I_0(x), \quad (3)$$

with

$$x = 2\sqrt{Z_K^1 Z_{\bar{K}}^1} = 2Z_K^1. \quad (4)$$

From (1) and (3) one can calculate the density n_K of particles with strangeness +1, the kaons, via the relation

$$n_K^{\text{gc}} = \frac{1}{V} \lambda_s \frac{\partial}{\partial \lambda_s} \ln Z^{\text{gc}} \Big|_{\lambda_s=1} = \frac{1}{V} \lambda_s Z_K^1 = \frac{Z_K^1}{V}, \quad (5)$$

and considering the canonical case one finds

$$\begin{aligned} n_K^c &= \frac{1}{V} \lambda_s \frac{\partial}{\partial \lambda_s} \ln Z^c \Big|_{\lambda_s=1} \\ &= \frac{1}{V} \frac{I_1(x)}{I_0(x)} \sqrt{\frac{Z_{\bar{K}}^1}{Z_K^1}} Z_K^1 = \eta n_K^{\text{gc}}, \end{aligned} \quad (6)$$

using that in the grand canonical picture $\langle N_K \rangle - \langle N_{\bar{K}} \rangle = 0$ requires $\lambda_s = \sqrt{Z_{\bar{K}}^1 / Z_K^1} = 1$.

Comparing (5) and (6), one defines the canonical suppression factor $0 \leq \eta \leq 1$

$$\eta = \frac{n_K^c}{n_K^{\text{gc}}} = \frac{I_1(x)}{I_0(x)}, \quad (7)$$

which contains all relevant information on differences in the equilibrium particle density between the grand canonical and canonical description.

An alternative way of understanding this suppression is to consider kinetic master equations [16,17] by looking at a single process $ab \leftrightarrow c\bar{c}$. $P_{N_c}(t)$ denotes the probability of finding N_c particles c at a time t . In our case we have $c \equiv K$ and thus $N_c = N_{\bar{c}}$ holds exactly, whereas particles a and b (the ‘‘pions’’) are assumed to be uncorrelated and abundant. Furthermore, the

probabilities for a single gain or loss process per unit time and volume are denoted by G/V and L/V , respectively, where $G = \langle \sigma_G v \rangle$ and $L = \langle \sigma_L v \rangle$ are the momentum-averaged cross sections for the gain and loss processes. With that, a master equation can be formulated [16]

$$\begin{aligned} \frac{dP_{N_c}}{dt} &= \frac{G}{V} \langle N_a \rangle \langle N_b \rangle P_{N_c-1} + \frac{L}{V} (N_c + 1)^2 P_{N_c+1} \\ &\quad - \frac{G}{V} \langle N_a \rangle \langle N_b \rangle P_{N_c} + \frac{L}{V} N_c^2 P_{N_c}. \end{aligned} \quad (8)$$

A general solution of this equation is possible [17], but for our purpose it is sufficient to look at the kinetic equation for the time evolution of the average number $\langle N_c \rangle$. It can be obtained when multiplying (8) by N_c and summing over it:

$$\frac{d\langle N_c \rangle}{dt} = \frac{G}{V} \langle N_a \rangle \langle N_b \rangle - \frac{L}{V} \langle N_c^2 \rangle. \quad (9)$$

This equation can be easily treated in the two limiting cases $\langle N_c \rangle \gg 1$ and $\langle N_c \rangle \ll 1$. For abundant production of $c\bar{c}$ pairs, i.e., when $\langle N_c \rangle \gg 1$, the relation $\langle N_c^2 \rangle \approx \langle N_c \rangle^2$ holds. However, for very rare production, i.e., when $\langle N_c \rangle \ll 1$, one has the relation $\langle N_c^2 \rangle \approx \langle N_c \rangle$. Assuming a thermal momentum distribution with

$$\frac{G}{L} = \frac{Z_c^1 Z_{\bar{c}}^1}{Z_a^1 Z_b^1}, \quad (10)$$

and looking at stationary solutions for large times (the solutions describing an equilibrated system), one ends up with ($\epsilon \equiv G \langle N_a \rangle \langle N_b \rangle / L$)

$$n_c = \frac{\langle N_c \rangle}{V} = \frac{\sqrt{\epsilon}}{V} = \frac{Z_c^1}{V} \equiv n_c^{\text{gc}} \quad (11)$$

for $\langle N_c \rangle \gg 1$. The opposite case $\langle N_c \rangle \ll 1$ leads to

$$n_c = \frac{\langle N_c \rangle}{V} = \frac{\epsilon}{V} = \frac{Z_c^1 Z_{\bar{c}}^1}{V} \equiv n_c^c. \quad (12)$$

Identifying particle-type c with kaons, it is clear that (11) equals the grand canonical result (5). Equation (12) is just the leading term in an expansion of the canonical result (6). Hence, it is verified that an abundant production of particles leads to a grand canonical description, whereas rare particle production requires a canonical description.

Let us have a closer look at the canonical suppression factor (7) using the asymptotic behaviors

$$\lim_{x \rightarrow \infty} \frac{I_1(x)}{I_0(x)} \rightarrow 1 \quad \text{and} \quad \lim_{x \rightarrow 0} \frac{I_1(x)}{I_0(x)} \rightarrow \frac{x}{2}. \quad (13)$$

Here, one sees that in the grand canonical limit the kaon density n_K is independent of the reaction volume, whereas in the canonical regime with the number of kaons $\langle N_K \rangle \ll 1$ it scales linearly with the volume as $x \propto V$. Figure 1 illustrates this behavior.

III. REAL TRANSPORT AND SIMULATION SETUP

The main objective of our study is to demonstrate that current (large scale) transport models are able to reproduce the effect of canonical suppression. This is not a trivial investigation. One might argue that the transport algorithms

are based on strictly solving the Boltzmann equation which in turn originates from a grand canonical treatment. In the stationary limit of the (coupled) Boltzmann equations the equilibrium phase space distributions, where the various collision terms for each particle population vanish, obey Maxwell-Boltzmann statistics (or Bose-Einstein or Fermi-Dirac statistics when the Pauli factors are included), so that the individual densities are that of a grand canonical ensemble. The reason for this is that when describing an annihilation within a Boltzmann description the two (rare) particles are assumed to be completely uncorrelated. This is, however, not the case in the description via the master equation (8). Here the occurrence of a pair of rare particles is explicitly taken care of. Because of the nature of pair production the existence of a kaon requires the existence of an antikaon. This leads to an effective increase in the annihilation process compared to the Boltzmann stosszahlansatz. Inspecting the loss term in (9), the approximation leading to a Boltzmann process is given by

$$\langle N_c^2 \rangle \xrightarrow{\text{Boltzmann process}} \langle N_c \rangle^2, \quad (14)$$

which then leads to the grand canonical description. Staying within the description of the master equation, the possibility for annihilation is much higher. When there exists a kaon, there must be an antikaon with which an annihilation process is possible. $\langle N_c^2 \rangle \gg \langle N_c \rangle^2$ for $\langle N_c \rangle \ll 1$; hence the effective annihilation rate incorporated correctly in the master equation is much larger than that for a Boltzmann description, leading to the canonical suppression.

Moreover the various numerical realizations of the underlying transport equations do conserve energy and the individual quantum charges (like baryon number and net strangeness) exactly—as within a microcanonical treatment. The argument of an “enhanced” annihilation should therefore also apply within these realizations. To address this question, we concentrate on the volume dependencies in the grand canonical and canonical regimes as depicted in Fig. 1.

The simulation setup consists of a large box of 20 fm side length holding a relativistic gas of pions. The pion gas provides a heat bath for a much smaller reaction volume of variable size centered within the large box. Inside this smaller and likewise box-shaped reaction volume processes $\pi\pi \leftrightarrow K\bar{K}$ are allowed, covering all possible isospin states of pions and kaons. The kaons are reflected by the walls of the small reaction volume and are thus bound to it, whereas these walls are permeable for the pions. An illustration of this special spatial setting is given in Fig. 2. After equilibration, the kaon density within the reaction volume should be governed by Eq. (6), which holds as a reference for the transport model results. The idea therefore is to simulate different sizes of the inner reaction volume and to extract the number of kaons $\langle N_K \rangle$ for each simulation run by averaging over many time steps to minimize the statistical fluctuations. These time steps are sufficiently separated to avoid correlations. Furthermore the data are taken after the equilibration of the system.

We implemented this scenario using two different types of transport descriptions—the microscopic transport model UrQMD [18,19] and a realization of a stochastic transport model borrowed from a recently developed parton cascade

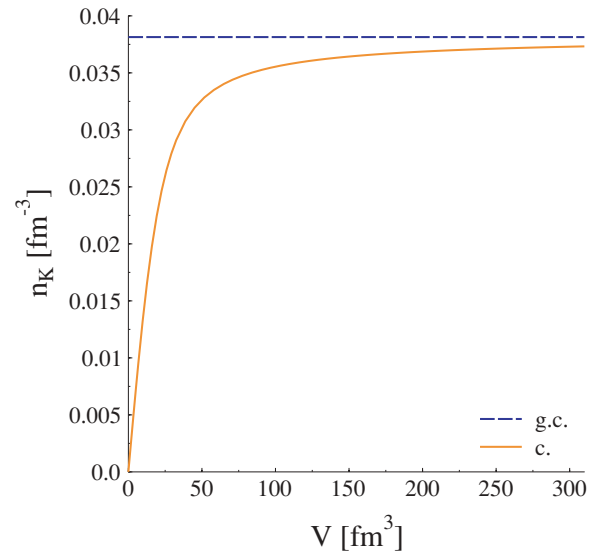


FIG. 1. (Color online) Volume dependence of the kaon density for a canonical ensemble [cf. Eq. (6)] for $T = 170$ MeV. g.c. denotes the grand canonical calculations; c. labels the canonical result.

[24]. The former model makes use of a geometrical interpretation of cross sections to solve the transport equations, whereas the latter relies on the explicit calculation of transition probabilities.

For standard applications, the UrQMD model provides full space time dynamics for hadrons and strings. It is a nonequilibrium model based on the covariant propagation of hadrons and strings. All cross sections are fitted to available data or calculated by the principle of detailed balance. For our studies the code is modified such that only reactions $\pi\pi \leftrightarrow K\bar{K}$, together with elastic collisions among the pions and kaons, remain possible. The $\pi\pi \rightarrow K\bar{K}$ inelastic reactions are

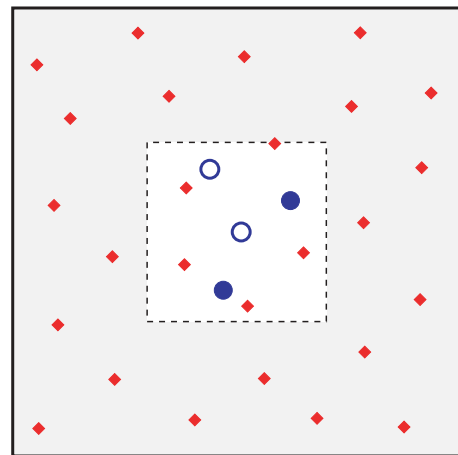


FIG. 2. (Color online) Illustration of the two boxes for the numerical simulation: The pions (diamonds) move inside the larger and fixed box and thus provide a heat bath for the kaons and antikaons (open and filled circles), which can only move and interact inside the small box. The size of the small box is varied for investigating the dynamical occurrence of canonical suppression in small volumes.

assigned a constant cross section of 1, 5, or 10 mb, whereas the backward reactions are calculated via the principle of detailed balance.

The simulation of $2 \leftrightarrow 2$ processes within the stochastic method is based on the calculation of a collision probability for each possible particle pair per unit volume Δ^3x and unit time Δt via [24]

$$P_{22} = v_{\text{rel}} \sigma_{22} \frac{\Delta t}{\Delta x^3}. \quad (15)$$

Here, v_{rel} denotes the relative velocity and σ_{22} is the cross section for the considered $2 \leftrightarrow 2$ process. Similar to the UrQMD setup, the cross sections are set to be constant in one direction and calculated via detailed balance for the reverse reaction. The so obtained probability is then compared with a random number between 0 and 1 to decide whether the collision does take place or not. The implementation of the stochastic model is therefore closely related to the formulation of the master equation (8) and its solution discussed in Sec. II. We must stress one important point: The stochastic method is, in principle, flexible to introduce test particles, that is, to “subdivide” each particle into a number N of test particles [24]. However, for the following investigation it is crucial that the produced kaons are *not* subdivided into further test particles. We discuss this further below.

The initial conditions in both schemes are chosen such that the pion gas acquires a temperature of $T = 170$ MeV. The appropriate number of pions and the total energy of the system are calculated via the use of a grand canonical partition function (1) for pions alone, as kaons are absent in the initial state. The total energy evaluates to

$$U(T, V) = \frac{g_\pi V}{2\pi^2} m_\pi^2 T^2 \left\{ 3K_2\left(\frac{m_\pi}{T}\right) + \frac{m_\pi}{T} K_1\left(\frac{m_\pi}{T}\right) \right\}. \quad (16)$$

A heat bath volume of 8000 fm^3 , as used in our simulations, then corresponds to a population of 1348 pions bearing a total energy of 747.5 GeV. Initially each pion is assigned the same fraction of the total energy, giving one half of the particles momenta in the positive x direction, while the remaining particles start out bearing momenta in the negative x direction. The spatial distribution is random.

IV. RESULTS FOR THE DYNAMICAL SUPPRESSION

A necessary verification of the simulations reliability is to check for kinetic equilibration. Figure 3 demonstrates that the energy distribution of the pions does become exponential over six orders of magnitude with the desired temperature of $T = 170$ MeV in both schemes.

Figures 4 and 5 now display the actual results in terms of the kaon density as a function of the (small) reaction volume. The minor fluctuations in the results indicate the small statistical errors due to the finite number of averages done. It is clear that the canonical suppression is reproduced by both transport schemes. The kaon yield is suppressed for small reaction volumes with respect to the grand canonical limit. This verification states the main result of the present study.

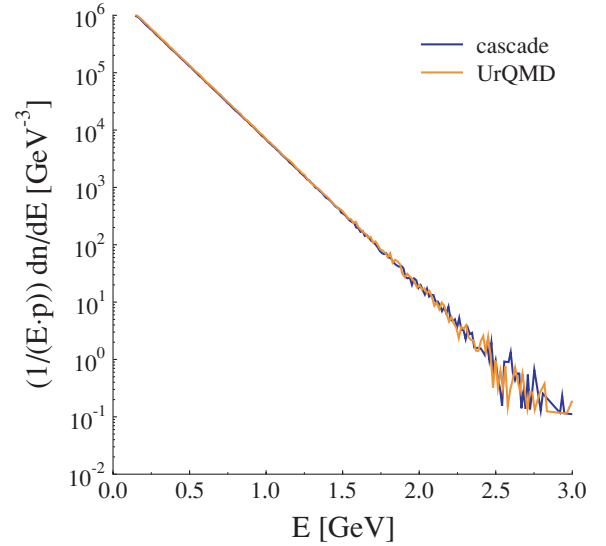


FIG. 3. (Color online) Logarithmic energy spectra for the pion gases within the UrQMD and cascade calculations. Both spectra are identical within statistical fluctuations.

In general, certain deviations from the theoretical values are to be expected because of the choice of initial conditions. Pion number and energy content are fixed such that, without any kaons present, the system is tuned to the reference temperature of $T = 170$ MeV and fugacity $\lambda = 1$. The production of the heavier kaons then leads to small changes in these parameters, as the total energy in the system is conserved as well as the total number of particles, because only particle number conserving

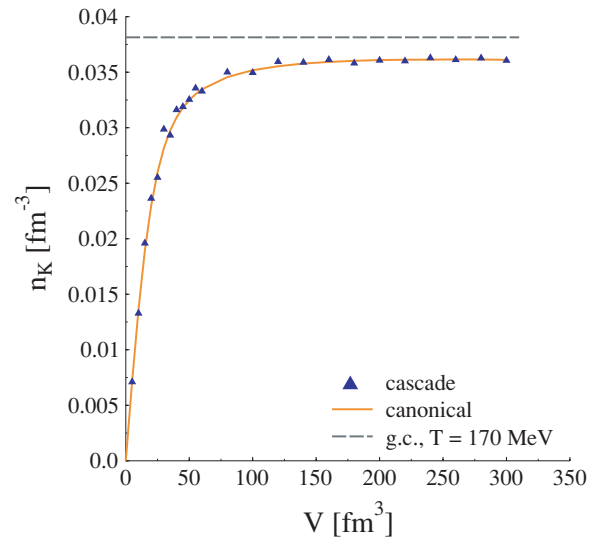


FIG. 4. (Color online) Kaon density versus reaction volume as extracted from simulations within the stochastic cascade (triangles). For comparison, the dashed line indicates the grand canonical behavior. The solid line shows the canonical volume dependence of the kaon density, based on (6) for a temperature of $T = 170$ MeV and corrected by taking small deviations in temperature and fugacity into account.

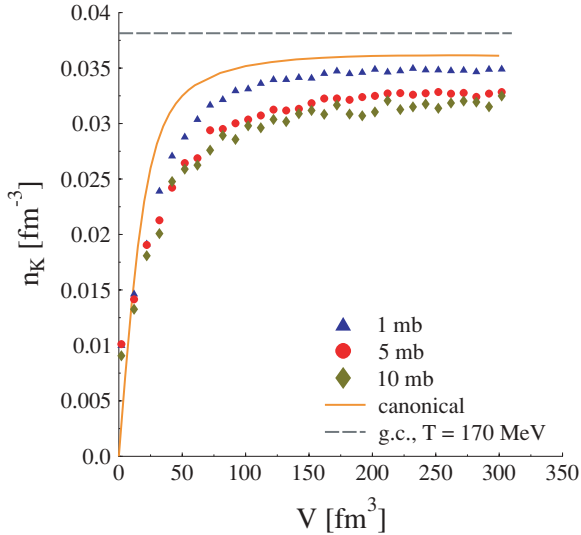


FIG. 5. (Color online) Kaon density versus reaction volume as extracted from simulations using the UrQMD model. Cross sections of 1mb (triangles), 5mb (circles), and 10mb (diamonds) were assigned to the forward direction of the inelastic reactions $\pi\pi \leftrightarrow K\bar{K}$. The solid and dashed lines again provide the theoretically expected behavior as seen in Fig. 4.

collision processes are included in the present study. This slightly affects the equilibrium number of pions and thus also the kaons. In the case of the stochastic cascade we investigated the relative deviations of temperature $T_{\text{new}} = T + \Delta T$ and effective mesonic fugacity $\lambda_{\text{eff}} = 1 + \Delta\lambda$ more closely. It was found that both deviations indeed grow with the number of kaons produced and thus with the size of the reaction volume. The observed deviations are on the order of 2% at most. Taking these deviations into account, the theoretical results can be adapted to the actual conditions present in the system at a given size of the reaction volume by rescaling with the effective fugacity factor. The actual theoretical reference curves in Figs. 4 and 5 are corrected that way.

The stronger deviations for the microscopical UrQMD model cannot be solely explained by the changes in temperature and fugacity. In fact, the crucial effect when using the geometrical concept of incorporating binary collisions is a decrease in the collision rate, when the expected mean free path $\lambda_{\text{m.f.p.}} = (n\sigma_{22})^{-1}$ for the particular reaction gets in the order of the interaction length $\sqrt{\sigma_{22}/\pi}$ as pointed out in [24]. This is due to the difference in the collision times of the involved particles viewed from the computational frame. During that interval the particle having the larger collision time must not collide again to ensure causality. Thus, the collision rate is decreased compared to the one given by the collision integral. As different densities are involved, one cannot expect forward and reverse reactions to be affected in the same way and the changes in reaction rates lead to a shifted stationary “equilibrium” value of the kaon density.

This behavior can be clearly seen in Fig. 5, where the kaon density is depicted for different cross sections of the forward reaction $\pi\pi \rightarrow K\bar{K}$. The smaller the chosen

cross section and thus the larger the mean free path, the more accurately the theoretical result is reproduced. On the contrary, for typical real mesonic cross section the numerical shortcoming is in the range of 10% to 15%. Please note that this deviation from the equilibrium value does not depend on the specific implementation of the $\pi\pi \leftrightarrow K\bar{K}$ process. We have also checked that the process $\pi\pi \leftrightarrow f_2 \leftrightarrow K\bar{K}$ with the proper energy-dependent cross sections leads to the same result.

Too few kaons relative to the pions are simulated in comparison to the theoretical limit either in the canonical or the grand canonical regime. Such a discrepancy in kaon number relative to the pion number with respect to experimental results has been reported in several URQMD calculations [25]. It might well be that a better implementation of the collision criteria will enhance the kaon relative to the pion yield. We leave this for a detailed future investigation.

Another instructive way to analyze the results is to look at the suppression factor η (7) as a function of the average number of kaons $\langle N_K \rangle^c$ present in the system. This relation is independent of the temperature, which can be easily shown: Because the suppression factor is a function of Z_K^1 , $\eta = \eta(Z_K^1)$, the one-body partition function can in principle be expressed in terms of η ,

$$Z_K^1 = Z_K^1(\eta), \quad (17)$$

which then leads to

$$\langle N_K \rangle^c = \eta \langle N_K \rangle^{\text{gc}} = \eta Z_K^1(\eta). \quad (18)$$

Figure 6 states the summary of the investigation and depicts the previous functional relation together with the simulation results. Here the temperature and fugacity deviations were taken into account for the cascade results. For the calculations employing the UrQMD model the suppression factor was calculated by taking the ratio of the actual kaon density

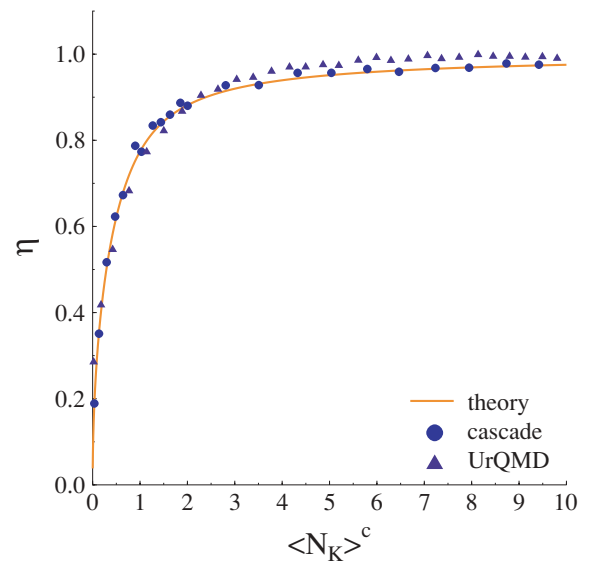


FIG. 6. (Color online) Suppression factor η as a function of the average kaon number.

$n_K(V)$ divided by the density $n_K(V \rightarrow \infty)$ in the limit of very large volumes. Within this prescription the sensitivity on the cross section vanishes almost completely. Apart from the demonstration of the excellent agreement between theory and simulation, the plot illustrates the two limiting cases considered when solving the kinetic equation (9). Small particle numbers $\langle N \rangle \ll 1$ are associated with the canonical regime, whereas for abundant particle production $\langle N \rangle \gg 1$ the grand canonical description is fully valid.

V. SUMMARY AND CONCLUSIONS

We have demonstrated that two current (large scale) transport models are able to reproduce the effect of canonical suppression. As a particular example we have chosen the production of kaons and antikaons via pions. The overall kaon yield is suppressed with respect to the grand canonical limit for small reaction volumes and thus small numbers of produced kaons.

The present transport algorithms are based on solving the Boltzmann equation with additional constraints; i.e., the solutions maintain the correlations due to charge, strangeness, and energy conservation. The canonical suppression for kaon numbers $\langle N_K \rangle$ considerably smaller than one, as pointed out in [16], originates dynamically from an enhancement of the annihilation process by $1/\langle N_K \rangle$ as compared to standard, grand canonical formulation of the Boltzmann equation. The reason is that any kaon in the system requires the existence of a corresponding antikaon due to strangeness conservation. Thus the probability of finding a particle-antiparticle pair turns into a highly correlated conditional probability compared to that obtained via the uncorrelated Boltzmann stosszahlansatz. The so enhanced annihilation probability then leads to the canonical suppression in the kaon yields. As the calculations show, it is manifest that the occurrence of canonical suppression is dynamically reproduced by the two presented schemes for solving the kinetic transport equations. A small discrepancy, i.e., a slightly lower kaon yield on the order of 10 to 15%, is present when employing typical cross sections. This discrepancy can be traced back to the numerical realization of the occurrence of collisions via the standard geometrical description. Deviations of the same order of magnitude $\sim 10\%$ – 20% are also encountered for other produced particle species and in the collision rates. As already emphasized, detailed investigations within the UrQMD model are in order to clarify how important such effects are for the understanding of kaon yields in relativistic heavy ion collisions, as typically too few kaons are produced relative to the pions, when compared to experimental results [25].

Addressing especially the dynamical generation of canonical suppression, one has to worry about even more significant violations when other numerical transport schemes are invoked. One popular scheme is the so called test-particle method; i.e., each real particle is subdivided into N test particles to obtain smoother distributions or to suppress other numerical artefacts (see, e.g. Ref. [24]). When applying this idea of particle subdivision to the stochastic method, it will rescale the volumes V of Fig. 4 by a factor $1/N$, so that the

grand canonical limit is achieved for much smaller volumes. This is, of course, unphysical. Thus, whenever the canonical suppression is of relevance for the understanding of particular yields, the test-particle method must be avoided.

Another often applied method is the so called perturbative method with “virtual” particles (for a discussion, see [26]). Here it is assumed that the exotic particles being produced are so rare that their behavior does not alter the overall dynamics. If the backreaction of kaon production, i.e., the annihilation of a kaon and its antiparticle, is not considered correctly, then detailed balance is violated and the system can never achieve full and correct chemical equilibrium.

When simulating real heavy ion collisions to address the production of kaons for lower or moderate relativistic energies (for a very recent work, see [27]), one has indeed to worry whether these backreactions are important in the sense that the rates necessary to achieve chemical equilibrium are smaller or comparable to the overall lifetime of the fireball. Various applications of thermal models for such low energies have been put forward in several works over the last years for describing hadronic yields in heavy ion collisions at SIS [13–15,28]. As only very few yields are available, the soundness of such an analysis is not evident. In principle, such an analysis rests on the assumption that chemical equilibrium among the individual hadronic particles is temporarily achieved, which implies that the corresponding time scales are sufficiently short compared to the lifetime of the fireball.

From transport theory residing on binary elastic and inelastic hadronic collisions, it has been known for a long time that for intermediate to moderate energies the kaons are predominantly produced before the initial motion is substantially degraded and when the system is still far from any (quasi-)equilibrium stage (for a discussion and review, see [29]). Putting it differently, when the momenta of the nucleons are sufficiently degraded and the system has to some extent thermalized, the time scale for production of strange particles via the considered inelastic kinetic reactions becomes extremely large. For a particular calculation in a static environment at somewhat larger energies, it was found that the equilibration of the kaons is exceeding the lifetime of a potential fireball by at least two orders of magnitude [30]. In this analysis the comparison was made, however, to a grand canonical estimate.

Yet, as we argue now, a chemical equilibrium situation of kaons with canonical suppression included cannot be achieved even temporarily when assuming known cross sections. Within a grand canonical environment the rate for chemical equilibration of a particle C for a reaction of type $A + B \leftrightarrow C + D$ is given by $\tau^{-1} \approx \langle \sigma_{CD} v_{CD} \rangle n_D$, where n_D is the particle density of species D . With $n_K = n_{\bar{K}}$, if there is only one kaon, then there also has to exist one antikaon in the particular realization of the system. Hence, for such a situation of a canonical realization, where the reactions $\pi + \pi \leftrightarrow K + \bar{K}$ will drive the kaons to chemical equilibrium, the subsequent equilibration rate is obtained by substituting for n_D the effective antikaon density $1/V$. The rate thus reads

$$\tau_{\text{chem},K}^{-1} \approx \langle \sigma_{K\bar{K} \rightarrow \pi\pi} v_{K\bar{K}} \rangle \frac{1}{V}. \quad (19)$$

In a UrQMD simulation the typical averaged cross section rather close to threshold is given by $\langle\sigma_{K\bar{K}\rightarrow\pi\pi}v_{K\bar{K}}\rangle\approx 2$ mb, so that $\tau_{\text{chem};K}\approx 5V/(\text{fm}^2c)$. Any typical reaction volume at intermediate time scales in a relativistic heavy ion reaction is on the order of 100 fm^3 . Hence, kaons cannot be expected to come or stay close to chemical equilibrium.

ACKNOWLEDGMENTS

The authors thank S. Leupold and U. Mosel for discussions, which have stimulated this work. This work is supported by GSI, DFG, and BMBF. The computational resources have been provided by the Center for Scientific Computing in Frankfurt.

-
- [1] E. Fermi, *Prog. Theor. Phys.* **5**, 570 (1950); *Phys. Rev.* **81** 683 (1951).
- [2] L. D. Landau, *Izv. Akad. Nauk Ser. Fiz.* **17**, 51 (1953).
- [3] R. Hagedorn, *Nucl. Phys.* **B24**, 93 (1970).
- [4] P. J. Siemens and J. I. Kapusta, *Phys. Rev. Lett.* **43**, 1486 (1979).
- [5] A. Z. Mekjian, *Nucl. Phys.* **A384**, 492 (1982).
- [6] D. Hahn and H. Stöcker, *Nucl. Phys.* **A476**, 718 (1988).
- [7] P. Braun-Munzinger, J. Stachel, J. P. Wessels, and N. Xu, *Phys. Lett.* **B365**, 1 (1996).
- [8] P. Braun-Munzinger, D. Magestro, K. Redlich, and J. Stachel, *Phys. Lett.* **B518**, 41 (2001).
- [9] P. Braun-Munzinger, K. Redlich, and J. Stachel, To appear in *Quark Gluon Plasma 3*, edited by R. C. Hwa and Xin-Nian Wang, World Scientific Publishing; arXiv:nucl-th/0304013.
- [10] J. Rafelski and M. Danos, *Phys. Lett.* **B97**, 279 (1980).
- [11] P. Koch, J. Rafelski, and W. Greiner, *Phys. Lett.* **B123**, 151 (1983).
- [12] R. Hagedorn and K. Redlich, *Z. Phys. C* **27**, 541 (1985).
- [13] J. Cleymans, D. Elliott, A. Keranen, and E. Suhonen, *Phys. Rev. C* **57**, 3319 (1998).
- [14] J. Cleymans, H. Oeschler, and K. Redlich, *Phys. Rev. C* **59**, 1663 (1999).
- [15] H. Oeschler, *J. Phys. G* **27**, 257 (2001).
- [16] C. M. Ko, V. Koch, Z. W. Lin, K. Redlich, M. Stephanov, and X. N. Wang, *Phys. Rev. Lett.* **86**, 5438 (2001).
- [17] K. Redlich, V. Koch, and A. Tounsi, *Nucl. Phys.* **A702**, 326 (2002).
- [18] S. A. Bass *et al.*, *Prog. Part. Nucl. Phys.* **41**, 225 (1998).
- [19] M. Bleicher *et al.*, *J. Phys. G* **25**, 1859 (1999).
- [20] M. Belkacem *et al.*, *Phys. Rev. C* **58**, 1727 (1998).
- [21] L. V. Bravina *et al.*, *Phys. Rev. C* **60**, 024904 (1999).
- [22] L. V. Bravina, E. E. Zabrodin, S. A. Bass, M. Bleicher, M. Brandstetter, A. Faessler, C. Fuchs, W. Greiner, S. Soff, and H. Stöcker, *Phys. Rev. C* **63**, 064902 (2001).
- [23] L. V. Bravina, E. E. Zabrodin, S. A. Bass, M. Bleicher, M. Brandstetter, S. Soff, H. Stöcker, and W. Greiner, *Phys. Rev. C* **62**, 064906 (2000).
- [24] Z. Xu and C. Greiner, *Phys. Rev. C* **71**, 064901 (2005).
- [25] E. L. Bratkovskaya, M. Bleicher, M. Reiter, S. Soff, H. Stöcker, M. van Leeuwen, S. A. Bass, and W. Cassing, *Phys. Rev. C* **69**, 054907 (2004).
- [26] C. Hartnack, Extract from habilitation thesis, arXiv:nucl-th/0507002.
- [27] A. B. Larionov and U. Mosel, *Phys. Rev. C* **72**, 014901 (2005).
- [28] R. Auerbeck, R. Holzmann, V. Metag, and R. S. Simon, *Phys. Rev. C* **67**, 024903 (2003).
- [29] C. Greiner, *J. Phys. G* **28**, 1631 (2002).
- [30] E. L. Bratkovskaya, W. Cassing, C. Greiner, M. Effenberger, U. Mosel, and A. Sibirtsev, *Nucl. Phys.* **A675**, 661 (2000).